Field Maxima
Inside Habitable Structures
Exposed to 2.45 GHz
Plane Wave Radiation

H. J. Liebe

TABLE OF CONTENTS

Page

LIST OF FIGURES

LIST OF TABLES

EXECUTIVE SUMMARY

It is necessary for the EMC analysis of the SPS to know microwave field strengths that would be expected inside various structures, particularly buildings and vehicles. Theoretically, such structures could concentrate incident microwave energy to produce fields more intense than would otherwise be expected. Very little work has been done explicitly on this problem, but a substantial body of theoretical and experimental information is available on the coupling of microwaves into enclosures and their behavior therein. An exact, detailed analysis of the microwave properties of habitable structures is not practical due to the tremendous variety of materials and complex geometries involved.

The problem of estimating the fields inside habitable structures exposed to microwaves near an SPS rectenna is analyzed in this report, with particular attention to the possibility of increases in field strength. This study describes and discusses relevant physical processes, lists measured values for many of the quantities involved, and cites actual microwave field strengths measured inside houses exposed to 2.6 GHz radiation from a satellite. Key results are summarized below.

To determine microwave field strengths inside a structure, the coupling of energy into the structure and its behavior inside, including reflections (possibly resonant), must be understood. Coupling to the interior could occur via relatively microwave-transparent openings (windows, for example) or through wall materials, which in general do not transmit microwaves as well. The following approximate microwave transmissions for representative structural elements have been measured:

| | % Transmission | |
Structure	Dry	Wet
Wooden Wall	15	6
Frame Wall	40	15
Window (wood sash)	70	40

Metal walls or screening, or even foil, transmits very little 2.45-GHz microwave energy (less than 1%) if openings or joints are substantially less than an inch long.

Average field strengths inside structures are expected to be less than those outside, due to coupling losses. The structure could, however, alter the spatial distribution of energy to produce localized areas of increased field intensity. Reflections within structures are the most likely causes of locally-increased field strength. Metallic surfaces are the most common elements of habitable structures likely to produce significant field increases. In the absence of any absorbing material, a single metallic reflection could increase power density at some locations by as much as a factor of four above that incident on the surface. More complex geometries involving multiple reflections could, in principle, produce larger field increases. However, such large increases require special geometries and very little microwave absorption in the system. Neither of these criteria is likely to be satisfied by real habitable structures. In particular it should be noted that the presence of people, who are significant microwave absorbers and reflectors, modifies reflection patterns in a time-varying way as the people move and absorb energy, reducing the field increases possible due to reflections.

Measurements have been reported giving the ratio of microwave field strength inside to that outside single family houses illuminated by 2.6 GHz microwaves from a satellite (Wells, 1977). Average fields inside were found to be about 25% of those outside, although interior fields varied substantially from point to point. For the case of highest ratio of average inside fields to outside fields, the probability of encountering a microwave field inside that was larger than that outside was only 15%. If, in specific cases, interior microwave field strengths were found to be a problem, they could easily be reduced by methods described in the present report.

FIELD MAXIMA INSIDE HABITABLE STRUCTURES EXPOSED TO 2.45 GHz PLANE WAVE RADIATION

Hans J. Liebe*

This report discusses microwave engineering data relevant to assess the potential of the Satellite Power System (SPS) to cause microwave field enhancements (so-called "hot spots") inside habitable structures (house, trailer, car, etc.) located in the fringe area of the receiving rectenna. Mitigative measures are included in the discussion.

1. INTRODUCTION

In feasibility studies of the SPS microwave energy beaming concept, the question was raised whether local free space field strength maxima (hot spots) inside habitable structures located in the fringe area of the receiving rectenna can exceed the uniform power density of the incident free space plane wave radiation. The answer lies in the quantitative assessment of penetration, storage, and dissipation of field energy into and within the space surrounded by a lossy dielectric (e.g., house), metallic (e.g., vehicle, airplane), or composite dielectric-metallic (e.g., trailer) shell.

The many parameters of the problem (electromagnetic properties of building material, furnishings, biota; geometric shapes, openings, and dimensions; outside and inside obstructions; etc.) make it virtually impossible to predict the internal field distribution with certainty by analytical means. As in many complicated problems, attempts are made to simplify the analysis by considering subproblems which can be treated independently. The final answer is then looked upon as a combination of such solutions. The following sub-areas (including some key words for variables and/or effects) are considered:

1. Incident Radiation (power density distribution, obstruction loss, polarization, and elevation angle dependences).

2. Interaction with the Exterior (reflection, diffraction, scattering, and absorption effects by the outer shell of the structure).

3. Penetration of SPS Field Energy into the Interior (three coupling mechanisms: direct, aperture, diffuse).

---

*The author is with the U.S. Department of Commerce, National Telecommunications and Information Administration, Institute for Telecommunication Sciences, Boulder, Colorado 80303.

4. Possible Field Maxima (multiple reflections; excitation of resonances; dissipation of resonant energy; the empty, furnished, occupied chamber).

1.1. The Incident Microwave Radiation Field

The SPS field incident upon a habitable structure is assumed to be a coherent plane wave with linear vertical polarization. The proposed frequency is in the UHF range at

$$f_o = 2.45 \text{ GHz} \quad \text{or} \quad \lambda_o = 12.2 \text{ cm} \tag{1}$$

for the wavelength in free space. The direction of propagation is to the south (geostationary orbit; i.e., equator plane) with elevation angles

$$\phi = 30° \text{ to } 60° \tag{2}$$

for the continental United States. The proposed maximum power density S_o at the beam center is

$$S_o = 23 \text{ mW/cm}^2 = 230 \text{ W/m}^2, \tag{3}$$

and it is the valid index of a plane-wave field apart from phase, polarization, and direction (Wacker and Bowman, 1971). The energy density (3) compares with other known ones as follows (in units of mW/cm^2):

2×10^{-4}	moon light
10^{-6} to 10^{-3}	UHF radio radiation in an urban area
<0.1	fringe area of SPS rectenna
10	current U.S. standard for maximum continuous microwave exposure level (acceptable thermal burden for humans)
23	SPS maximum power density (3)
120	sunlight on a clear day (50% IR, 40% visible, 10% UV)
10^3	localized microwave therapy
2×10^5	microwave cooking
1.2×10^{10}	breakdown of sea level atmosphere (ionization).

The power density incident in the fringes of the receiving site (see Appendix A for complete power density pattern) is given by

$$S = S_0 \ 10^{-0.1L} = E^2/2Z_0 \qquad W/m^2 \tag{4}$$

(E is the peak electric field amplitude, $Z_0 = 377\Omega$ is the characteristic free space impedance), where L (dB) is the average power reduction factor as a function of the radial distance from the beam axis (Appendix A):

r (km)	0	5	10	20	50
L (dB)	0	15	24	33	43.

The incident field might be further reduced by obstructions causing diffraction loss (e.g., trees located close to a housing structure). The diffraction edge for trees in full leaf was measured at 2.95 GHz to coincide with the physical height (LaGrone, 1977). In this case, the knife edge diffraction approximation can be used yielding additional 3 to 30 dB reductions in the effective power density S.

1.2.   Formulation of the Hot Spot Problem*

The electromagnetic field within a habitable structure is expressed via its electric field components interacting with dielectric and metallic material. The free space field distribution in chambers, such as rooms in a house, cockpit of a vehicle, cabin of an aircraft, etc., is to be investigated for local field energy maxima (hot spots) E_i^2. For a point with the internal space coordinates x, y, z, one can define

$$E_i^2 = E_x^2 + E_y^2 + E_z^2 \qquad (V/m)^2 \tag{5}$$

and write a maximum power transmission coefficient to be (see equation 4)

$$q_i = E_i^2/E^2 \quad . \tag{6}$$

The objective of this study is to identify and, if possible, to quantify situations that might exhibit a field Hot Spot Problem (HSP) defined by

$$q_i > 1 \quad . \tag{7}$$

---

*The term "hot spot" is used for a local electric field maximum; for the resulting thermal effect see equation (26).

3

Such a condition can exist within a volume element as small as $(0.5 \lambda_0)^3$ assuming the maximum spatial periodicity between field maxima and minima to be $\lambda_0/4$. Even before discussing the various electromagnetic effects that might lead to $q_i > 1$, one has to take note of the complexity of the problem by pointing to the fact that an average habitable space has a large number of potential hot spots (e.g., the room size 4 x 5 x 2.5 m has about 2×10^5 possibilities).

Reflections of the incident radiation from intercepting surfaces are the key to assessing the likelihood of a HSP. *Single reflections* from curves surfaces can focus plane wave fields into spots, and *multiple reflections* can lead to resonant standing wave patterns with locally well defined field concentrations.

The total power P available to cause effects is that "seen" by the shadow cross section X cast by a structure exposed to SPS radiation and is given simply by

$$P = SX \qquad W \quad . \tag{8}$$

The shadow area X is typically between 5 and 500 m^2; the power density S in the fringe area of the rectenna is not expected to exceed 0.1 mW/cm^2 (see Appendix A), hence the total maximum exposure power falls in the range

$$P_0 \approx 5 \text{ to } 500 \text{ W} \qquad . \tag{9}$$

"Worst" cases would exist when (a) all of the power P_0 is focussed into "one" spot such as is the case for a parabolic or spherical reflector with an on-axis or offset focal point or when (b) the power P_0 is used to sustain a low loss resonance field. Neither condition, however, will occur inside a habitable structure since both have to be very carefully engineered for such purposes to ensure "perfect" reflections and "perfect" geometries.

The following discussion will concentrate on the field energy that is consumed in the interior space of a structure, which is only a part of the total P (8). One can divide the cross section X into three components,

$$P = S(X_s + X_t + X_i) \qquad W \qquad , \tag{10}$$

where the contribution denoted SX_s is lost by reflection and absorption on the outside of the structure, the component SX_t describes the loss via transmission through the structure into the ground, and only $P_i = SX_i$ is the power dissipated in the interior space.

4

Enhanced field strength is best understood by considering the simple case of a direct and a reflected plane-wave signal interfering with each other. Enhancement occurs at all points in space where direct and reflected wave fronts differ in phase by multiples of 2π. A HSP exists when an arrangement of reflecting surfaces supports multiple reflections allowing a standing wave (resonance) field to build up. The phase relationship between direct and reflected monochromatic (f_0) signals will be influenced by the size and shape of the enclosure, by the presence and location of objects and persons, and by the position of the test point.

A practical resonator stores electromagnetic energy at the resonance frequency f_r and, simultaneously, suffers a power loss P_r from conduction, dielectric, and diffraction effects. Two dimensionless factors can be defined to describe the resonance case. They are the quality- or Q-factor,

$$Q = 2\pi(\text{energy stored})/P_r \quad , \tag{11}$$

and the coupling coefficient,

$$q \equiv \frac{\text{energy available to sustain a resonance field}}{\text{total energy available } (SX_i)} \tag{12}$$

One speaks of a resonance when

$$Q > 1 \quad . \tag{13}$$

With respect to a field strength maximum E_0 of a resonance within habitable space, we assume the following:

1) Only part of the penetrated energy SX_i is coupled to support a resonance field which yields for (12) that

$$q < 1 \quad . \tag{14}$$

2) Any local maximum E_0 of the resonance field is enhanced by the quality factor Q over the field energy $qE_i^2 = q_i\, qE^2$, which excites the resonance.

3) The field strength is distributed around the resonance frequency f_r according to

$$E_0 \sim Q/(1 + a^2) \quad \text{V/m} \quad , \tag{15}$$

where the frequency is normalized to $a = 2Q(f_0 - f_r)/f_r$ in multiples of the resonance halfwidth $f_r/2Q$ with reference to the SPS frequency f_0.

A HSP condition $T > 1$ exists when the reductions by coupling (q_i, q) and detuning ($f_o - f_r$) are overcome by the field enhancement QE_i. The resonance case leads for (7) to the reformulation

$$T = (E_{HSP}/E)^2 \qquad q_i \ q[Q/(1 + a^2)]^2 \qquad . \tag{16}$$

At this point, let's briefly reiterate the train of thought that led to the array of variables introduced in equations (1) through (16). The first step is to find the incident power density S, which determines with (4) the exposure field strength E. Next, the coupling $q_i \leq 1$ (6) into a chamber is specified and followed by an identification of inner surfaces that might support multiple reflections at or close to f_o. Then, the effective Q-factor of the resonance and the coupling q to the internal field strength E_i are estimated. For example, r = 10 km, L = 24 + 6 (tree shading) dB, S = 0.23 W/m^2, E = 13 V/m; direct coupling (window), $q_i \approx 0.9$; resonance between two metal partitions with $Q \approx 4$ at $f_r = f_o$ and a coupling factor of q = 0.05. It follows from (16) that there would be no HSP ($T \approx 0.7$).

To obtain a more reliable assessment of a HSP, one needs to conduct a careful appraisal of field characteristics pertinent to specific reflector configurations in terms of their electromagnetic properties (reflection coefficient, resonance condition, dielectric constant, loss tangent, etc.). The identification of all arrangements which support enhanced or resonant fields based on available theoretical and experimental knowledge for the innumerable configurations is an impossible task. Real hot spot conditions can only be verified by "in situ" measurements in suspected areas.

The following sections are intended as a fact-finding exercise to sketch properties of a 2.45 GHz field within habitable space in simplistic terms to bring out basic principles, while more detailed discussions of the points raised can be found in the references.

2. MICROWAVE COUPLING INTO AN ENCLOSURE

The coupling (6) of microwave radiation involves factors that scale with wavelength. There are basically two ways to enter an enclosure. The first is to radiate through natural openings (e.g., windows, open access holes, cracks, etc.); the other is to penetrate through the surrounding walls. The interior energy SX_i depends in a complicated manner on aperture size, polarization and angle-of-arrival for the incident wave, and on the electromagnetic properties

of the walls. A great deal of work has been done on the coupling problem in context with EMP (electromagnetic pulse due to a nuclear explosion) effects (Butler et al., 1978, and 166 references therein). The treatment of aperture coupling distinguishes two cases depending upon the relation of the largest aperture dimension d with respect to the wavelength λ_o:

(1) $d > \lambda_o$, direct coupling, and

(2) $d \le \lambda_o/2$, aperture coupling .

2.1. Direct Coupling

A sufficient approximation for apertures with dimensions larger than the wavelength λ_o is to equate the coupled energy P_i with the incident field energy SX and assume for the cross-section X the surface area A of the opening. This yields simply that

$$q_i = 1 \quad \text{and} \quad P_i = SA \quad W \quad . \tag{17}$$

Theoretical calculations of the coupling through circular, elliptical, and rectangular cross sections confirmed (17) (e.g., Koch and Kolbig, 1968). An example of q_i for a circular aperture is given in Figure 1 as a function of $(2d/\lambda) > 2$ (d is the diameter).

2.2. Aperture Coupling

When the largest dimension d of an aperture falls below $\lambda_o/2 = 6$ cm, the analysis of the coupled field energy is more complicated (Butler et al., 1978; Jaggard, 1977). The coefficient q_i can vary between zero and 1.7 (Figure 1); however, the total energy transmitted will be small (e.g., S = 0.23 W/m^2, A = $\lambda_o^2/4$ = 3.6·10^{-3} m^2, q < 2, P < 2 mW). Several noteworthy points are:

1. The electric field strength increases by as much as a factor of 5 at the edge of the aperture (Butler et al., 1978). An example is given in Figure 2.

2. The coupling reaches a maximum when $d \approx 0.4\ \lambda_o$. The increase to $q_i \approx 1.7$ (Figure 1) is explained by the fact that energy is collected from all angles over a hemisphere surrounding the aperture.

3. Maximum transmission through a circular aperture occurs for grazing incidence of a polarized plane wave; i.e., the magnetic field vector is aligned with the center axis (Jaggard, 1977).

7
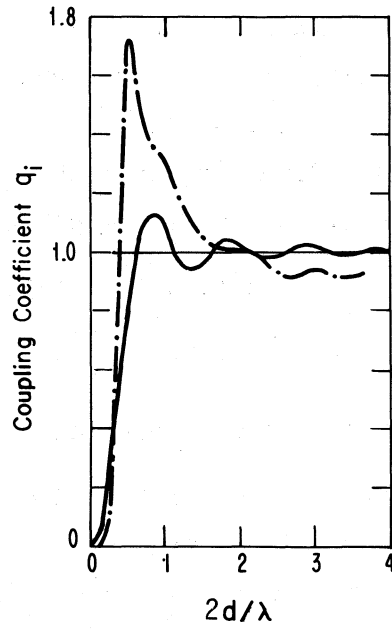
Figure 1. The coupling coefficient q_i of a circular aperture as a function of the diameter d/λ. Shown are the results of two different theoretical treatments (Koch and Kolbig, 1968)
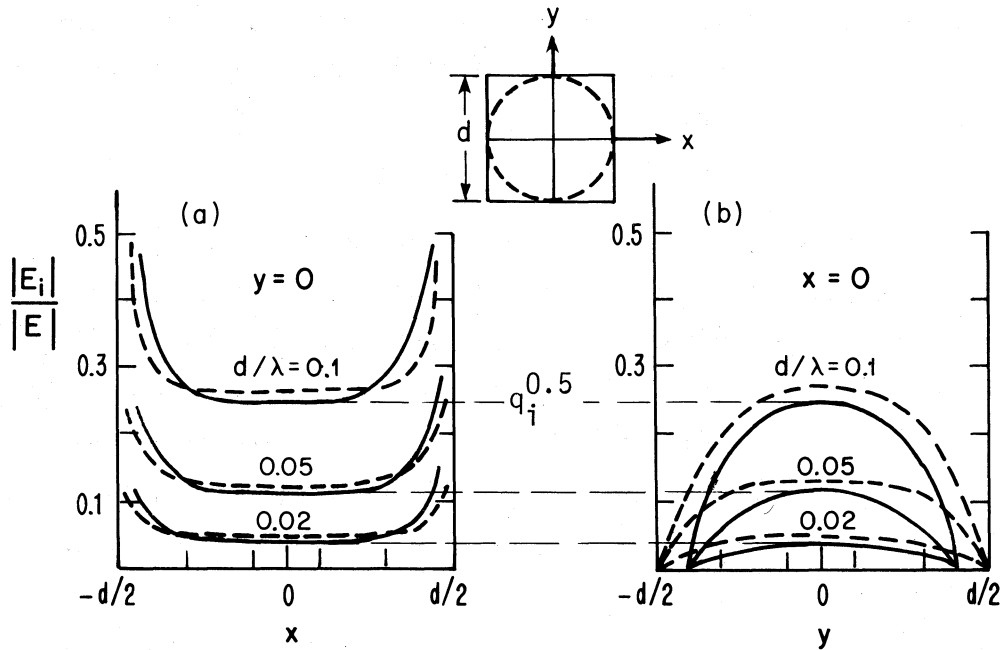
Figure 2. E_i-field distribution in circular and square apertures ($d \leq 0.1 \lambda$) excited by an E_x-field

(a) E_i field sampled along x-axis

(b) E_i field sampled along y-axis

(Butler et al., 1978)

4. In an array of apertures (e.g., windows along the fuselage of an aircraft), the coupling increases when the line of apertures is parallel to the incident magnetic field vector (Jaggard, 1977).

2.3. Diffuse Coupling

Microwave energy can penetrate into a cavity by means of "diffusion" through the walls when the wall conductivity is finite (Lee and Bedrosian, 1979). A wall is considered electrically "thin" when the skin depth δ is larger than the wall thickness d (see equation 21). A few measurements have been reported on the insertion loss L_i of typical composite building materials and are listed in Table 1.

Table 1. Measured Insertion Loss of Building Materials (Wells et al., 1975; private communication)*

	Loss L_i, dB		Frequency, GHz
	dry	wet	
Wooden wall	8	− 12	3.3
Frame wall	4 (5.3)	8	3.3 (4.7)
9" Brick wall + insulation + plaster	1.5	− 4	1.1
Window, wooden sash	1.5	− 3	3.3
Window, leaded panes	13		3.3

Diffuse coupling plays a major role with nonmetallic structures. The total exposure power SX (8) will be attenuated; however, the amount reaching the inner space could still be substantial and contribute to a hot spot problem should field concentrating devices exist internally.

3. INTERNAL REFLECTIONS

Reflections from the enclosure walls significantly affect the field distribution inside. The local energy density will be greater than obtained in free space when, at a test point, the majority of reflected energy is of proper phase to add to the energy arriving directly. The phase of a reflected signal and hence the local power density both are extremely sensitive to:

> size and shape of the enclosure,
>
> location of the test point,
>
> presence and location of objects (e.g., furniture, etc.) and persons.

---

*Wells, P. I., D. A. Hill, A. G. Longley, R. G. FitzGerrell, L. L. Haidle, and D. V. Glen (1975), An experiment design for the measurement of building attenuation, OT Technical Memorandum 75-199.

A substantial amount of reflected energy will radiate out through the same aperture (e.g., window, door, etc.) through which the incident energy came.

Determination of the reflectivity level in an enclosure is understood by considering the simple case of a direct-path plane-wave signal E_D (constant magnitude and phase) combining with an interfering plane-wave signal E_R arriving at the test point under an angle ϕ (see Figure 3). A maximum is produced by two wave fronts whose phases differ by 2π. The maximum amplitude is

$$E_{max} = E_D + E_R \quad V/m \tag{18}$$

and the angle ϕ is given by

$$\phi = \sin^{-1}(\lambda/p) \quad . \tag{19}$$

The spatial periodicity "p" depends upon the angle between the interfering wave fronts. The resulting field will form a standing-wave pattern with field maxima twice the value of the incident wave if a once-reflected signal does not suffer losses, that is

$$E_{max} = 2E_i \quad V/m \quad . \tag{20}$$

The field strength E_{max} and the periodicity p are altered when several wave fronts with different reflection angles ϕ interfere. Two examples of super-imposing space harmonics are depicted in Figure 4.

3.1. Reflective Losses from Metals

A surface with high reflectivity for the SPS microwave radiation consists typically of metal, of wire mesh (mesh size < 1.5 cm), or of a multilayer arrangement of low-loss dielectric plates (Harvey, 1970), whereby the dielectric multilayer reflector is unlikely to occur in habitable structures.

Metals reflect microwaves and conduct field-induced currents. A very small fraction of the incident energy is absorbed by the metal surface. The loss in one reflection is (f in GHz)

$$a_r = 4.19 \times 10^{-3} f \delta \quad \% \quad , \tag{21}$$

where the skin depth δ in μm is the distance the field strength has fallen to $1/e = 0.368$ of its surface value. In nonmagnetic metals,

$$\delta = 15.9 \times 10^3 / \sqrt{\sigma_M f} \quad \mu m \quad , \tag{22}$$

10
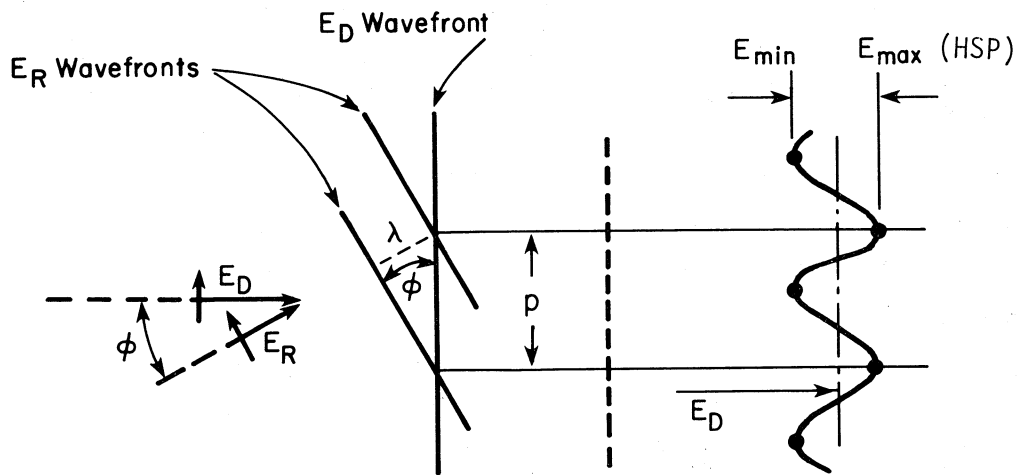
Figure 3. Spatial interference pattern due to a reflected wave

E_D - direct ray

E_R - field from specular reflection

p - spatial periodicity

(Crawford, 1974)
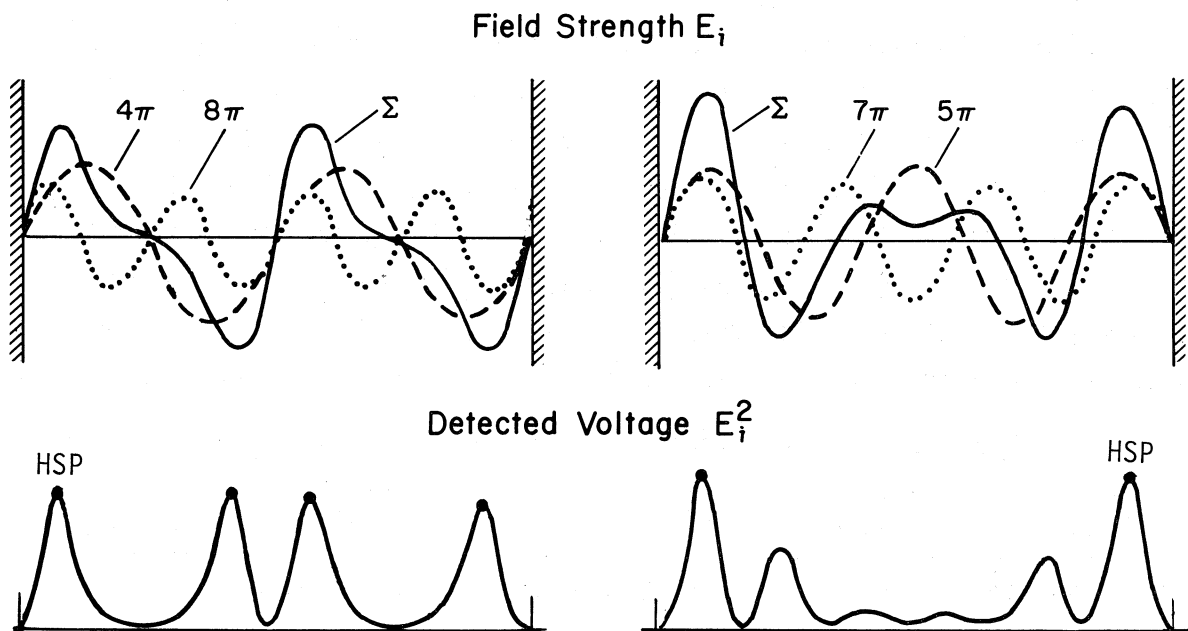
Figure 4. Two examples of field patterns between two opposing plate reflectors for the case that two space harmonics superimpose

Table 2. Reflective Properties of Metals (2 GHz)

Metal	Conductivity σ_M, (mho/m)10^6	Skin Depth δ, μm	Reflective Loss a_r, %
Aluminum	38.2	1.82	0.0152
Brass (66-34)	25.6	2.2	0.0185
Chromium	38.5	1.8	0.0151
Copper	58.1	1.48	0.0124
Gold	41.0	1.76	0.0148
Platinum	9.52	3.65	0.0307
Silver	61.7	1.43	0.0120
Steel	22.7	2.5	0.0210
Tin	8.8	3.80	0.0319

with σ_M being the conductivity in Siemens (mho) per meter (see Table 2). The calculated values of a_r in Table 2 are greater than measured values by a typical factor of two; however, all metal surfaces are excellent reflectors for SPS radiation.

Bare metal surfaces of significant area will be rare within the confinement of habitable boundaries. The chamber material, instead, which reflects, absorbs, and transmits the field can be anisotropic and, in addition, it can be non-stationary varying the field in space or time or both. Such media are difficult to deal with from the standpoint of solving the reflection problem. Already the general case of oblique incidence on a lossy homogeneous material is quite complicated. To gain some handle on the rather loosely defined term "habitable structure", we categorize it in Table 3 by means of the enclosure material, and look first at the microwave properties of lossy dielectric material.

Table 3. Electromagnetic Enclosure Properties

Case	Enclosure Properties	Coupling	Real Structure Equivalent
1	lossy dielectric	diffuse, aperture	brick, frame, stone house
2	composite of lossy dielectric and metal	aperture, diffuse	trailer, house with metal sidings, industrial building
3	metal plus dielectric coating	aperture	vehicle interior, aircraft cabin

3.2. Absorption and Reflection by Dielectric Material

Habitable space may be made from metals and other materials such as complex arrangements of natural and artificial dielectric materials. Dielectrics are a storage medium for field energy and dissipate such energy by conduction and other irreversible processes [e.g., volume inhomogeneity scatter (Roth and Clachi, 1975)]. Two frequency-dependent, dimensionless quantities,

$$\text{the relative dielectric constant} \quad K \quad (1 \text{ to } 80) \quad , \tag{23}$$
$$\text{and the loss tangent} \quad D \quad (0 \text{ to } 10) \quad ,$$

are needed to calculate conductivity, heat loss, and attenuation rate. An appreciable interaction effect occurs when the thickness of the material is larger than $\lambda_0/4 \approx 3$ cm. The wavelength in the medium is shortened by

$$\lambda_D = \lambda_0/\sqrt{K} \quad \text{cm} \quad . \tag{24}$$

The dielectric quantities K and D of materials related to habitable structures are given in the following Section 3.3.

The dielectric conductivity is obtained from

$$\sigma_D = 0.0556 \ f \ KD \quad \text{mho/m} \quad . \tag{25}$$

Values of 10^{-4} are typical for insulators, while semiconductors fall in the range of 10^2 mho/m.

In dielectric heating, the power absorbed per unit volume of material follows from

$$P_D = \sigma_D \ (E^2_{x,y,z})/2 \quad W/m^3 \quad , \tag{26}$$

being a function of position. The power attenuation rate is expressed by (VonHippel, 1954)

$$\alpha = 1.29 \ f \left\{ K \left[\sqrt{1 + D^2} - 1 \right] \right\}^{1/2} \quad \text{dB/cm} \quad , \tag{27}$$

and covers at f_0 the ranges given in Table 4.

Table 4. Power Attenuation Rate in Dielectric Material at 2.5 GHz

Relative Dielectric Constant K

		1	2	5	10	20
		α in dB/cm				
Loss Tangent D	10^{-3}	0.002	0.003	0.005	0.008	0.010
	10^{-2}	0.024	0.034	0.052	0.075	0.10
	10^{-1}	0.24	0.34	0.52	0.75	1.0
	1	2.2	3.0	4.7	6.8	9.1
	10	10	14	21	31	43

Reflections - Upon striking the surface of a dielectric material, the incident field is split into two components of which one is reflected and the other passes through the medium. Specular reflections from a smooth surface cause the angle θ of the reflected wave front to be equal to angle of incidence (Snell's law). For the HSP of interest, the amount of reflected energy is expressed by

$$\rho^2 = (E_r/E_i)^2 \quad , \tag{28}$$

where ρ is the reflection coefficient. We learned that for metals $\rho = 1$, for practical purposes (Table 2). In case of dielectric material, ρ becomes a function of wave polarization, angle of incidence θ, and the properties K and D.

Relatively simple expressions exist for the special case $D \approx 0$ (loss-free dielectric), where two different situations occur depending upon the orientation of the E_i-vector with respect to the plane of incidence:

(i) E_i is in the plane of incidence,

(ii) E_i is perpendicular to the plane of incidence.

For reflection on a horizontal surface, this means that for (i) the wave is horizontally and for (ii) vertically polarized. The respective reflection coefficients are (VonHippel, 1954)

14

$$\text{(i)} \qquad\qquad\qquad\qquad \text{(ii)}$$

$$\rho_h \doteq \frac{1-\sqrt{K}\cos\theta}{1+\sqrt{K}\cos\theta} \qquad \text{and} \qquad \rho_v = \frac{\cos\theta-\sqrt{K-\sin^2\theta}}{\cos\theta+\sqrt{K-\sin^2\theta}} \qquad\qquad (29)$$

For normal and zero incidence, $\rho_h = \rho_v$; in all other cases, $\rho_h > \rho_v$. At the special angle (Brewster) $\theta_B = \tan^{-1}\sqrt{K}$, all reflections are avoided for case (i), i.e., $\rho_h = 0$. In practice one can expect partial reflections $(\rho < 1)$.

Returning to the picture of reflecting and interfering rays and disregarding the shape of the boundary, it follows that the resulting field amplitude enhancement (free space SWR, to be measured along three orthogonal axes of the interior space) can be significant only when repeated reflections with little loss occur. Figure 5 gives three examples of geometries that are in principle capable of sustaining multiple reflections. The point-to-point free space SWR of two interfering wave fronts can be made plausible with the simple phasor diagram depicted and evaluated in Table 5. The actual ratio within a chamber will be extremely dependent on position due to the complex variation of the reflected signals. Experimental results have shown spatial variations of electric field strength as great as $\pm$ 40 dB in a room with bare metal surfaces (Donaldson et al., 1978).

Depolarization is another effect which is counter to a HSP. The extent of depolarization of incident radiation in habitable space is a function of the complexity of the confinement. Obstacles will scatter omnidirectionally, thus mixing vertical and horizontal field components to become equal. Even oblique reflections from dielectric-coated metal surfaces can depolarize a wave train. For example, a lacquer paint ($K \approx 10$) with a thickness of 0.04 mm causes a decrease in the cross polarization isolation (19 GHz, $\theta = 45°$) between vertical and horizontal from 40 to 36 dB (Chu and Semplak, 1976).

3.3. Dielectric Properties of Typical Materials

This section lists dielectric data of material that might be associated with habitable structures. The data summarized in Tables 6 to 9 were obtained from a survey of the sources referenced (VonHippel, 1954; Wells et al., 1975;
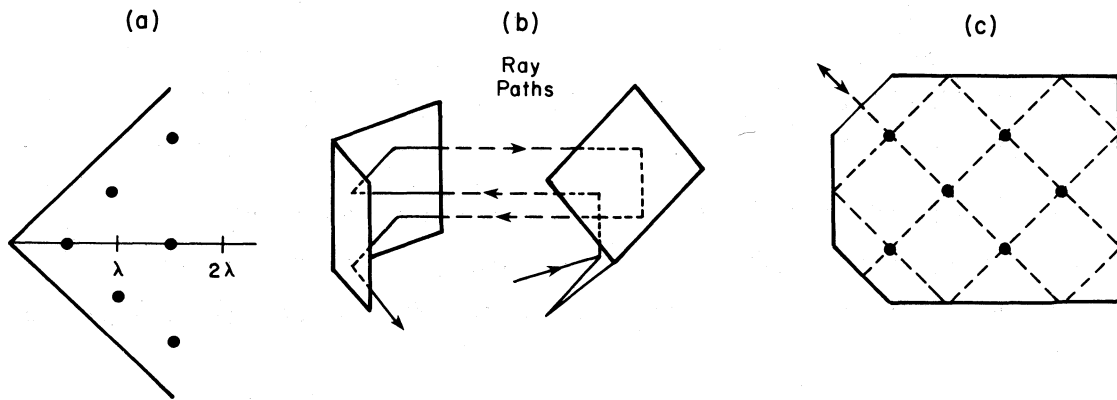
Figure 5. Two-dimensional metal reflector arrangements with the potential of supporting multiple reflections

    (a)   Hot spots near 90° corner reflector

    (b)   Opposing folded metal surfaces

    (c)   Closed multi-angled box with aperture (Harvey, 1970)

Table 5. Conversion Table for Return Loss α_r, Reflection Coefficient ρ, Standing Wave Radio SWR, and Peak-to-Peak Field Stength Variations (1±x) Relative to Unity Reference.
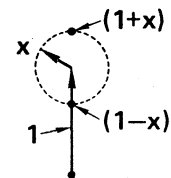
α_r	ρ	SWR	1+x	1-x	Remark
dB			dB	dB	
1	0.891	17.391	5.535	-19.27	
3	0.708	5.848	4.650	-10.69	HSP
6	0.501	3.010	3.529	-6.041	Possible
10	0.316	1.925	2.387	-3.302	
12	0.251	1.671	1.947	-2.513	
15	0.178	1.433	1.422	-1.701	
20	0.100	1.222	0.828	-0.915	
25	0.056	1.119	0.475	-0.503	
30	0.032	1.065	0.270	-0.279	
40	0.010	1.020	0.086	-0.087	Anechoic
50	0.003	1.006	0.027	-0.028	Chamber
60	0.001	1.002	0.009	-0.009	

Emerson, 1973; Donaldson et al., 1978; Emslie et al., 1975), most notable from the comprehensive treatment by VonHippel. For a HSP, we look after material that is a good reflector K > 3) and has a small loss tangent (D < 0.01). Low loss dielectrics (Table 6) are artificial materials normally not common in habitable structures but especially developed for microwave applications. The materials commonly used to construct habitable space are more or less lossy (see examples listed in Table 7).

Table 6. Low Loss Dielectrics (D < 0.01, f = 3 GHz)

	K	D		K	D
Fused Quartz	3.78	0.00006	Phosphate Glass	4.9 to 5.2	0.0018 to 0.0046
Styrofoam	1.03	0.00010	Borosilicate Glass	4 to 8	0.0012 to 0.0058
Teflon	2.1	0.00015	Corning 7070 Glass	3.9	0.0031
Polystyrene	2.55	0.00033	Lucite	2.58	0.0035
Butyl Rubber	2.35	0.0009	Plexiglas	2.60	0.0057
Porcelain	8.9	0.0011	Phenolic Board	1.19	0.0058
Polyglass D	3.23	0.0012			

Water is a very lossy dielectric, and the water content of materials determines to a large extent their dielectric behavior such as attenuation α (27) and reflectivity ρ (29). Water plays a role on the outside of habitable structures where it acts as a weather-variable shield. Also, the high water content of biota turns them into significant absorbers and reflectors. Their dielectric effects are simulated by a 4 percent aqueous salt (NaCl) solution. Reported dielectric properties of water are in Table 8; water content-dependent properties of various building materials are given in Table 9 and Figure 6.

Wooden structures will allow a certain amount of diffuse coupling (see 2.3), while window areas are good direct-coupling apertures (2.1) with partial reflections on both sides.

Table 7. Lossy Dielectrics (D > 0.01, f = 3 GHz)

	K			D		
Alkali Glass	4.8	to	6.0	0.005	to	0.012
Balsa			1.22	0.010		
Soda Glass	5	to	7.5	0.01	to	0.02
Nylon 66			3.03	0.013		
Granite	4.8	to	6.3	0.014	to	0.03
Poplar			1.50	0.015		
Plywood			1.5	0.022		
Silicone Rubber			5.7	0.025		
Shellac			2.86	0.025		
Mahogany			1.88	0.025		
Araldite			3.09	0.027		
Fir			1.82	0.027		
Fiberglass			4.4	0.029		
Birch			2.13	0.033		
Polyglass			4.86	0.034		
Nylon 610			2.94	0.036		
Bakelite			3.7	0.044		
Buna Rubber			2.45	0.044		
Neoprene			2.84	0.048		
Paper			2.70	0.056		
Formica			3.57	0.060		
Artifical Absorber Material	5	to	25	0.1	to	10

Table 8. Dielectric Properties of Water at 3 GHz

Pure Water	Temperature, °C	0	20	40
	K	81	78	73
	D	0.31	0.17	0.11
Salt Solution	NaCl-content, %	0	2	4
20° C	K	78	70	60
	D	0.17	0.38	0.55
Solid State		Ice (-20°C)	Snow (-6° C)	
	K	1.9	1.1 to 1.5	
	D	0.0014	0.0003 to 0.001	

Table 9. Dielectric Properties of Various Building
Materials Reported at 3 GHz

		Dry	Wet	
Sand, loam	K	2.5	20	(15% water)
	D	0.001-0.006	0.13	
Clay	K	2.3	11.3	(20% water)
	D	0.015	0.25	
Magnetite	K	1.0	30	(11% water)
	D	0.10	0.32	
Brick wall	α	0.5	0.7	dB/cm
Wooden panel	α	0.5-1	1-2	dB/cm
Roofing shingles	α	1.1-2.7	3.3-3.6	dB/cm
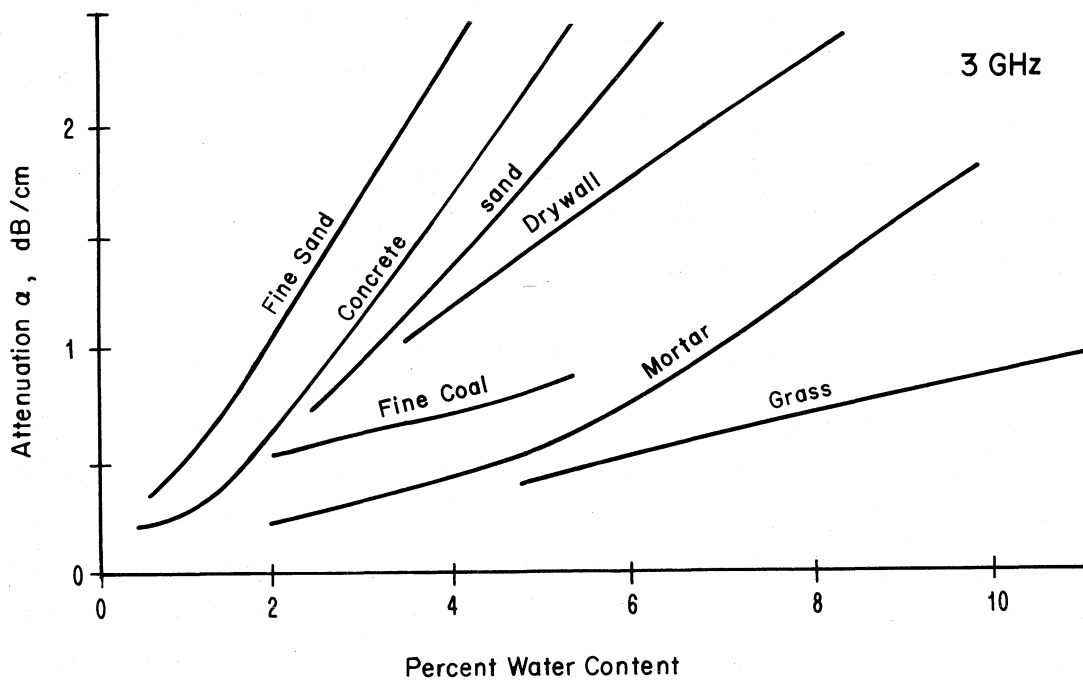
Figure 6. Attenuation rate α of various materials at 3 GHz as
a function of the water content.

4. POSSIBLE RESONANCE CHARACTERISTICS OF HABITABLE SPACE

The term resonance implies the existence of reflective boundaries and the build-up of high field amplitudes (equation 15) by multiple reflections. A standing-wave field alternates between electric and magnetic energy storage and is sustained by the energy coupled into the resonator. The Q-factor (11) can be calculated for simple cases (Appendix B) or determined, for example, by exciting a resonant structure with pulsed microwaves and measuring the ringing time τ yielding

$$Q = 2\pi f_r \tau \quad . \tag{30}$$

After the time τ, the energy content of the resonance has dropped to $1/e$ of its starting value.

4.1. Cavity Resonator

In general, any closed and somewhat reflecting cavity will support resonances regardless of its shape if only its dimensions are fixed and large compared to the wavelength λ_o. In most cases such conditions are met by habitable space.

The spectrum of possible resonances for a given λ_o becomes increasingly dense with growing cavity dimensions. The number of allowed resonance modes for a given geometry (see examples in Appendix B), the so-called "mode density", is approximately given by (Wilson et al., 1946, Kinzer and Wilson, 1947)

$$N_V \approx 8V/\lambda_o^3 \quad \text{for a cavity of volume V} \quad . \tag{31}$$

For example, a room of the size $4 \times 5 \times 2.5 = 50 \text{ m}^3$ can exhibit, in principle, on the order of $N_V \approx 2.3 \times 10^5$ resonance ($\lambda_o = 12$ cm) modes. These modes are expected to exhibit low Q-factors (Q < 10) in houses owing to the fact that walls usually are made from dielectric materials and reflect only part of the incident wave. Metal walls on the other hand are subject to ohmic (field-induced currents) and dielectric losses (wall coatings). In addition, the presence of lossy interior objects will dampen the resonance field.

The field distributions of the following cavity shapes have been calculated rigorously (Harvey, 1970):

(a) rectangular box, which most closely resembles a typical room,

(b) circular cylinder,

(c) spheres,

(d) elliptical cylinders,

(e) conical, toroidal, and cigar shapes,

(f) confocal spheroids and paraboloids.

The field equations for the geometries (a) to (c) are given in Appendix B. Case 3 (Table 3) might resemble to some degree one of these geometries. Theoretically, the peak value of the stored field energy density in an aperture-excited cavity can be up to two orders of magnitude above the incident value (e.g., Safari-Naini et al., 1977). Losses in a practical configuration, however, make a HSP very unlikely. The effective Q-value is calculated from

$$1/Q = (1/Q_W) + (1/Q_A) + (1/Q_M) \quad , \tag{32}$$

where the ratio between time-averaged field energy and (a) power dissipated in the walls by conduction loss (Q_W), and (b) power radiated out through the aperture (Q_A), and (c) dielectric heating loss by material in the cavity (Q_M) defines the individual quality factors. Large apertures cause a low value for Q_A (roughly the ratio between enclosure and aperture area). The ratio is close to one for vehicles. In aircrafts, the enclosure-to-aperture ratio is on the order of 10 to 100.

4.2. Open Resonator

For Case 2 (Table 3), a resonant wave field can be sustained by caustic shapes of two bounding, reflective surfaces, while free space provides the missing confining boundary. The mode density for an open resonator is (Weinstein, 1969)

$$N_s \approx 12 \, X_1/\lambda_0^2 \quad , \tag{33}$$

where X_1 is the effective area. A pair of opposing metal surfaces having an area of 1 m^2 can support up to 800 modes at f_0.

Practical configurations of open resonators are innumerable (e.g., Weinstein, 1969; Schulten, 1976; Auchterlonie and Ahmed, 1977). Some of the simpler cases are depicted in Figure 7. These configurations support the more interesting modes with small radiation losses. Their mode patterns can be represented by two beams of rays propagating in opposite directions without losing energy through transverse radiation. The Q-factor of a resonance is determined by radiation loss due to diffraction out of the bounding surfaces and by conduction loss within them. Open resonator Q-values are very susceptible to misalignments of the ideal geometry. High Q-values afford little tolerance to dimensional changes. For example, in the case of a plane parallel mirror pair, a deviation by as small as $\lambda_0/100$ from being equidistant drops the Q-value to below 10 from the value on the order of 10,000 for a "perfect" geometry. The stringent accuracy requirements make a HSP due to open resonators unlikely. Some geometries are less sensitive (self-focusing) than others to misalignments. For example, two square ($\approx 10\lambda$ x 10λ) aluminum sheets slightly but arbitrarily bent in a crossed cylinder arrangement had fairly high ($> 10^2$) Q-factors (Schiffman, 1970; see Figure 7g).

4.3. Modeling of Resonance Fields

The limited time available for this study did not permit giving the modeling aspect of HSP more than a cursory glance. To remedy some of these shortcomings, the references covering relevant topics might be consulted.

Modeling the field distribution of resonances in habitable space has its place to identify "worst" case situations. Since the peak value of the stored energy varies rapidly with position, calculations at a very large number of locations will be required (Safari-Naini et al., 1977). While the model should accurately describe the resonant field distribution leading to a HSP, it will also contain a lot of conjecture and simplification about the real situation. It is logical to proceed as follows:

1. Examine the possibility of resonant modes in a given structure assuming perfectly reflecting walls.

2. Consider the excitation chances for these modes via coupling to the incident field energy.

3. Introduce losses resulting (a) from imperfect specular or diffuse reflections, (b) from metallic or dielectric conduction, (c) from
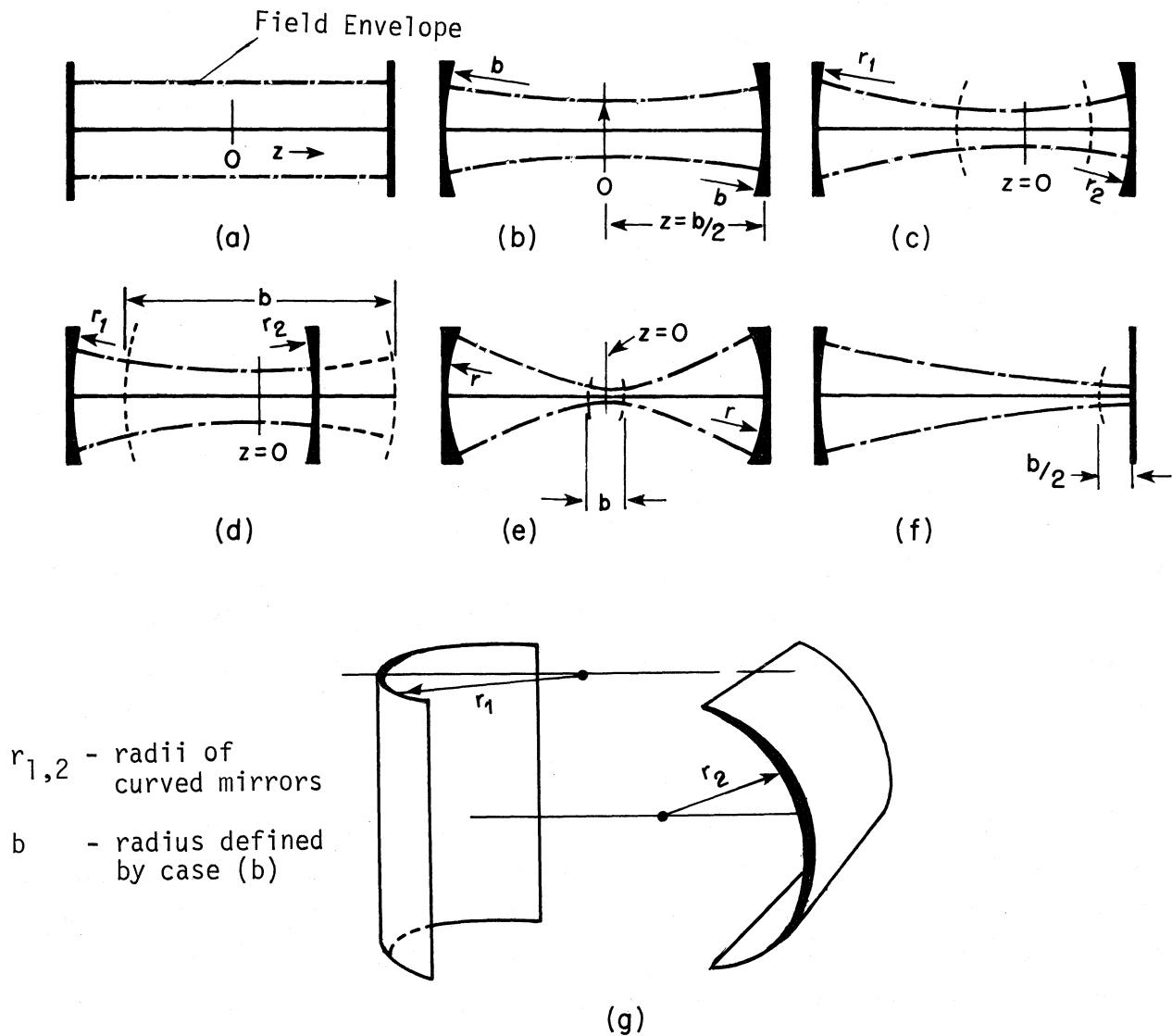
Figure 7. Examples of open resonator geometries (Harvey, 1970; Schiffman, 1970; Weinstein, 1969)

(a) Plane parallel

(b) Symmetrical confocal

(c) General spherical

(d) Asymmetric confocal

(e) Concentric

(f) Semi-confocal

(g) Crossed cylinders

diffraction and aperture radiation, and (d) from the presence of furnishings and biota.

4. Superimpose all possible resonant modes to the composite field pattern.

To complicate matters further, a possibility exists for latent resonances; i.e., resonances that are tuned in by a dielectric object moving within the enclosure. A person inside a resonant cavity will cause a perturbation of the resonance properties roughly proportional to the filling factor k_1, which is defined by one-half the ratio between body and cavity volumes. The effective Q-factor (32) and shift in resonance frequency are approximately

$$1/Q_{eff} \approx (1/Q) + k_1 D \quad \text{and} \quad f_r' \approx f_r(1 - k_1 K) \quad . \tag{34}$$

The combination of loss and high dielectric constant ($D \approx 0.5$, $K \approx 60$) makes the chances of sustaining a resonance in a small room very remote. For one person, the ratio k_1 will vary typically between 10^{-1} (e.g., cabin of a vehicle) and $<10^{-4}$ (e.g., large hall).

5. MEASUREMENTS

No systematic measurements of a HSP in habitable structures have been reported, and only a few data on internal signal strength have been gathered at microwave frequencies. In some cases, these results were compared with values taken simultaneously on the outside to define a building penetration loss L_r for the purpose of assessing signal coverage inside buildings. In those instances, the mean value for L_r was always positive (see equation 4). The general consensus from these efforts was that such measurements are complicated by reflection, diffraction, and scattering both inside and outside the enclosure; that multipath effects cause signal level variations of about $\pm$ 20 dB (see Figure 8) when scanning across an arbitrary room axis; that these results are extremely sensitive to size and shape of the enclosure and the presence and location of furnishings and people; that normal incidence of incoming radiation produced the lowest penetration loss L_r; and that metals and glass with wire mesh effectively shielded the field.

The internal field E_i^2 (5) is best mapped with a miniature (dimensions $\leq 0.1\lambda$) isotropic probe and a scanning mechanism. By coupling the linear motion of the probe and the measured signal strength to a recorder, an interference pattern similar to SWR curves is obtained (Crawford, 1974). Amplitudes and periods of the recorded oscillations can be analyzed to locate the source of the interfering signal for mitigative measures.

24
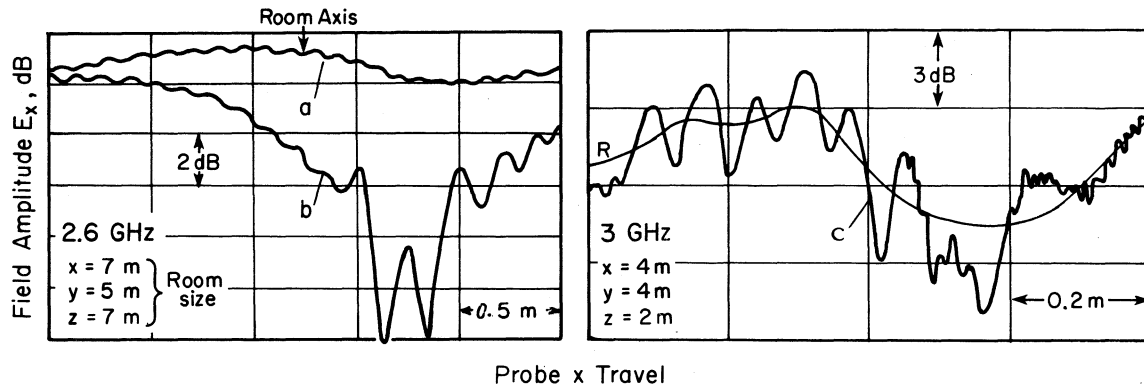
Figure 8. Examples of measured free space SWR (interference patterns)

 (a) Empty anechoic chamber

 (b) Anechoic chamber with structure in middle axis
   (Crawford, 1974)

 (c) Anechoic chamber with some absorbers removed
   (Appel-Hansen, 1973)

5.1. Strength of 2.6 GHz Satellite Signal Inside Houses

A recent extensive measurement series by Wells and Tryon (1976), and Wells (1977) of the 2.6 GHz signal strength (from the geostationary ATS-6 satellite beacon) inside 27 single-family houses across the continental United States comes the closest to assessing a HSP that we could find in an experimental study. The penetration loss L_r was determined by making spot measurements of the field strength in two rooms at two probe heights and eight randomly chosen locations both inside and outside a house. The details of the experiment design are reported by Wells et al., (1975) in a report of limited distribution (see footnote on page 9). The loss L_r was investigated as a function of construction type, climate, elevation angle, and room position with respect to the incoming radiation.

A statistical treatment of the data base revealed the following. The penetration loss for all cases was $L_r = 6.3 \pm 1.2$ dB. The average loss from case-to-case varied due to the position of the room in the house by $\pm$ 0.6 dB, due to the exterior construction material (e.g., wood, brick) by $\pm$ 1.2 dB, and due to the insulation in ceilings and walls by $\pm$ 1.6 dB. The polarization dependence was significant in that the relative horizontal component was about 1.8 dB greater than vertical. There was little change ($\pm$ 1 dB) in L_r with elevation angle ($\phi \approx 55°$ to $3°$).

25
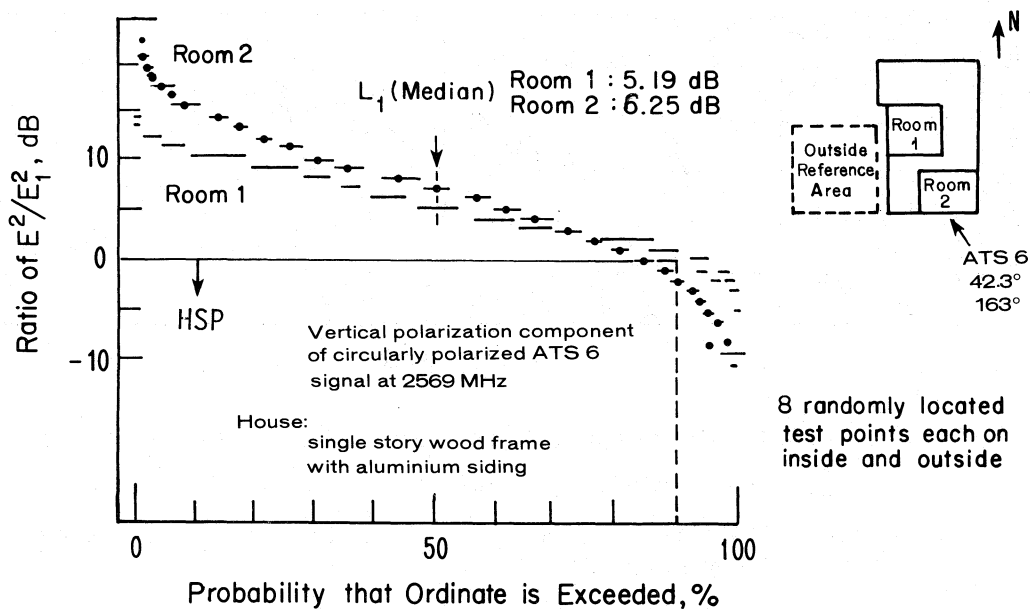
Figure 9. Probability distribution of hot spot occurrence inside single story wood frame house with metal sidings (worst case) exposed to a 2.57 GHz satellite signal (Wells and Tryon, 1976)

The variability of the inside signal level (e.g., $\pm$ 9 dB) was in all cases about twice as high as the outside reference level (e.g., $\pm$ 4 dB). Figure 9 gives the probability distribution of the individual L_r values for two rooms in a house (metal sidings, signal coupled through the roof) which had the lowest median for L_r (5.1 dB) of all houses measured. The 10 percent probability of a HSP occurring is insignificant in view of the large scatter of the data points.

5.2. Fields in Anechoic Chambers

The reflectivity level in anechoic chambers has been studied extensively for obvious reasons (Appel-Hansen, 1973; Crawford, 1974; Donaldson et al., 1978). A statistical sampling of data points (Wells and Tryon, 1976; Donaldson et al., 1978) is not sufficient to capture the complicated three-dimensional interference pattern. A free-space SWR probe has to be scanned along several orthogonal axes because a high degree of uncertainty exists about E_i (x, y, z). The examples in Figure 8 show that reflecting objects in the quiet zone or missing absorber material quickly deteriorate any low reflectivity level. The local maxima are

indicative of hot spots; however, in this case, the reference to an outer incident field (see equation 7) is missing. In principle, it is possible to locate the source of reflections from a completely known spatial interference pattern, but finding that pattern at every point from a theoretical evaluation is prevented by the complicated problem of defining the reflecting boundaries.

5.3. Fields in Mine Tunnel (Dielectric Waveguide)

Cavity boundaries made of dielectric (K > 3), low-loss (D < 0.02) material can guide SPS microwave radiation in any number of modes when the inner dimensions are larger than λ_o. All of these modes are lossy (typically between 0.02 and 0.5 dB/m at 2.5 GHz) since a dielectric wall is not a perfect reflector. Detailed electric field distributions have been measured, for example, in mine tunnels (e.g., Emslie et al., 1975). The lowest attenuation rates are those when, in geometric optics terms, the wavefront impinges upon a reflecting boundary with small grazing angles. Even modes in this category display low Q-factors in closed tunnel chambers. A dielectric waveguide might guide SPS radiation to a resonance structure that otherwise is not coupled to the outside.

In summary of Sections 2 to 5, we can say that the analysis has fallen short of its purpose. Other than an awareness of the significance of certain inter-action processes (coupling, reflection, loss) which are essential to a HSP, no firm estimates of upper bounds and variabilities in the quantities entering equation (16) were obtained. This is mainly due to the almost infinite number of possible geometric space configurations for empty habitable space.

6. MITIGATIVE MEASURES FOR MICROWAVE HOT SPOTS

Two principal means exist to achieve certainty that there is no hot spot problem; namely, to avoid penetration into the interior and/or to secure a uniform internal field distribution. In other words, apertures of sizes in the range $\approx (0.3 \text{ to } 3)\lambda_0$ and low-loss, permeable building material are to be avoided at the exposure site to minimize the cross section X_i (10), and little stored field energy is accomplished by suppressing internal reflections [low Q-factors (11)]. To circumvent an overapplication of absorber material, one should perform in suspected spaces a three-dimensional field scan and make sure that the free field SWR is within limits (say about $\pm$ 6 dB, see Table 5) by judiciously placing absorbers and rearranging specular reflectors.

6.1. Outside Reflectors and Absorbers

Shielding is an effective way to reduce the cross section X_i (10) which defines the power dissipated in the interior space. Measures to accomplish this are as follows.

- Utilize natural obstructions (e.g., tree grove).

- Use high-reflectance surfaces for the outer shell (metal sidings) especially towards the south.

- Shade apertures with metal awnings or cover them with wire mesh. The insertion loss of wire mesh in copper or steel at 2.45 GHz is:

L_i, dB	44	51	58
Size, meshes/cm	7x7	9x9	11x11.

- Cover apertures with resistive sheet material or embed absorbing cord around the edges where the highest electric coupling field strength occurs (see Figure 2).

- Keep unnecessary openings (slots, cracks, etc.) away from the exposed side or keep them below 2 cm in size (then $q_i < 0.1$).

6.2. Inside Absorbers

Field uniformity is the desired objective for anechoic chambers and has been studied extensively (Appel-Hansen, 1973; Crawford, 1974; Emerson, 1973; Donaldson et al., 1978). In these applications, it is attempted to keep the free-field SWR below $\pm$ 0.5 dB (see Table 5). In the case of habitable space, one could lessen the SWR tolerance. The application of nonreflecting absorbers to exposed metal surfaces should be an effective measure to mitigate potential hot spots.

Absorbers provide nearly reflection-free surfaces by matching their impedance Z to the free-space value Z_o (4). They come in three basic types:

1. <u>Broad band</u> absorbers are typical in anechoic chambers. To be effective under all angles of incidence, they have to be shaped (e.g., cones) and mounted in thick layers ($d > 10\lambda$). Different absorber materials can be staggereu to reduce the thickness and improve matching.

2. <u>Resonance</u> absorbers are much thinner than the broad-band type by taking advantage of the coherency in radiation. They are well suited for SPS applications. Reflections at the surface are suppressed by canceling them with reflections from the conducting base when the thickness $\ell = \lambda_0/4$. Under this type fall the Salisbury Screen absorbers (used in radar applications) where the remaining front-face reflections are reduced by a resistive layer. Covering metallic surfaces results in a typical reduction in reflectivity by 25 dB (Emerson, 1973).

3. <u>Surface</u> absorbers are designed to attenuate field-induced surface currents. They are not as effective as the other two types since $\ell \ll \lambda$, but they are easy to apply as spray or paint.

6.3. Mode Scrambler

Uniformity can be achieved by perturbing the field both in time and space with a moving reflector (rotating vane, oscillating metal sheet, etc.) within the chamber. Such a mode stirrer tunes the enclosure through all possible resonant modes at the frequency f_0. The electric field will pass through the possible maxima E_0 for each sequentially excited mode, thus essentially "smoothing" any spatial field distribution.

If feasible, another suggestion for mitigative measures of field hot spots deals with the possibility of randomly frequency-modulating the SPS microwave carrier being the electronic equivalent to a mode scrambler.

7. CONCLUSIONS

Incident SPS microwave energy which falls outside the rectenna area upon habitable structures will penetrate their chambers via aperture and "diffusion" coupling. The concentration into field "hot spots" (i.e., exceeding the incident level) by focusing, caustic surfaces or by multiple reflection mechanisms is, in principle, possible; however, dielectric losses and scattering from odd-shaped obstacles, normally part of habitable space, should clutter any spatial field pattern.

The foregoing treatment dealt in an elementary way with coupling of field energy into an enclosure and its possible spatial redistribution in standing wave or resonance fields. It should be emphasized that habitable space presents a poorly defined EM problem and that the whole subject has not received much attention. We attribute the lack of theoretical field analyses to the over-whelming complexity of the enclosure-contents configurations. The presence of

29

dielectric loads in the enclosure creates situations with the potential of being a complicated resonant system with several coupled oscillations which can only be clarified by measurements.

Modeling of the internal field structure based on given geometric and structural situations seems to be useful for related one- and two-dimensional cases to gain general insights into the true nature of a three-dimensional problem. In first approximation, the methods of geometric optics are to be applied. The exact distribution of internal radiation requires the application of field theory (Maxwell's equations) for a meaningful interpretation of interference patterns, standing wave fields, hot and dead spots, reactive zones, etc.

Measurements of reflectivity levels in certain chambers will be required employing an isotropic field probe and a scanning mechanism. Such a probe responds equally to signals of any direction and polarization, but can also be switched to select orthogonal field components for the location of reflection sources which might cause a particular "hot spot" problem.

Simple mitigative measures can effectively suppress the onset of hot spots. If reflections of the 2.45 GHz radiation at the outside are enhanced by metal sidings, awnings, and screening of apertures and dampened on the inside by lossy walls of low reflectivity, lossy furniture, avoidance of bare, opposing metal surfaces, etc., one can expect with some certainty that there is no HSP at all points of the inner space. If one has to be absolutely sure, then field uniformity can be attained by perturbing the field with a mode stirrer (e.g., rotating vane, pulsating reflector, moving body) or by random FM modulation of the SPS microwave power, which requires a certain bandwidth for the energy beam.

In summary, in any type of habitable enclosure there will be a nonuniform field strength distribution due to reflected and scattered field components interfering with each other. Essential to field enhancements are multiple reflections in a resonance mode, which are then proportional to the product of a quality factor Q and a coupling coefficient q. For almost all practical purposes it was concluded that this product Eq. (16) will not exceed unity.

8. ACKNOWLEDGMENTS

9. REFERENCES

Appel-Hansen, J. (1973), Reflectivity level of radio anechoic chambers, IEEE Trans. AP-21 (4), 490-498.

Auchterlonie, L. J., and I. Y. Ahmed (1977), Microwave wideband open resonator of large aperture, J. Physics E-10, 691-694.

Butler, C. M., Y. R. Samii, and R. Mittra (1978), Electromagnetic penetration through apertures in conducting surfaces, IEEE Trans. EMC-20 (1), 82-93.

Chu, T. S., and R. A. Semplak (1976), A note on painted reflecting surfaces, IEEE Trans. AP-24 (1), 99-101.

Crawford, M. L. (1974), Evaluation of reflectivity level of anechoic chambers using isotropic, 3-dimensional probing, Proc. 1974 Internat. IEEE/AP-S Symposium, pp. 28-34.

Dickinson, R. M. (1978), The beamed power microwave transmitting antenna, IEEE Trans. MTT-26 (5), 335-340 (see Appendix A).

Donaldson, E. E., W. R. Free, D. W. Robertson, and J. A. Woody (1978), Field measurements made in an enclosure, Proc., IEEE 66 (4), 462-472.

Emerson, W. H. (1973), EM wave absorbers and anechoic chambers through the years, IEEE Trans. AP-21 (4), 484-490.

Emslie, A. G., R. L. Lagage, and P. F. Strong (1975), Theory of the propagation of UHF radio waves in coal mine tunnels, IEEE Trans. AP-23 (2), 192-305.

Harvey, A. F. (1970), Coherent light, published by Wiley-Interscience, London and New York.

Jaggard, D. L. (1977), Transmission through one or more small apertures of arbitrary shape, AFC-GL Interaction Notes, Note 323, September.

Kinzer, J. P., and I. G. Wilson (1947), Some results on cylindrical cavity resonators, Bell Syst. Techn. J. 26, 410-445.

Koch, G. F., and K. S. Kolbig (1968), The transmission coefficient of elliptical and rectangular apertures for electromagnetic waves, IEEE Trans. AP-16 (1), 78-83.

LaGrone, A. H. (1977), Propagation of UHF electromagnetic waves over a grove of trees in full leaf, IEEE Trans. AP-25 (6), 866-869.

Lee, K. S., and G. Bedrosian (1979), Diffuse EM penetration into metallic enclosures, IEEE Trans. AP-27 (2), 194-198.

Roth, L. E., and G. Clachi (1975), Coherent electromagnetic losses by scattering from volume inhomogeneities, IEEE Trans. AP-23 (5), 674-675.

Safari-Naini, S., S. W. Lee, and R. Mittra (1977), Transmission of an EM wave through the aperture of a cylindrical cavity, IEEE Trans. EMC-19 (2), 74-81.

Schiffman, B. M. (1970), Crossed cylinder microwave resonator, IEEE Trans. MTT-18 (8), 509-510.

Schulten, G. (1976), Mircrowave optical ring resonators, IEEE Trans. MTT-15 (1), 54-55.

VonHippel, A. R. (1954), Dielectric materials and applications, published by J. Wiley & Sons, New York, NY.

Wacker, P. F., and R. R. Bowman (1971), Quantifying hazardous electromagnetic fields: scientific basis and practical considerations, IEEE Trans. MTT-19 (2), 178-187.

Weinstein, L. A. (1969), Open resonators and open waveguides, published by The Golem Press, Boulder, CO.

Wells, P. I., and P. V. Tryon (1976), The attenuation of UHF radio signals by houses, Office of Telecom. Report 76-98, August (NTIS Access No. PB-258447).

Wells, P. I. (1977), The attenuation of UHF radio signals by houses, IEEE Trans. VT-26 (4), 358-362.

Wilson, I. G., and C. W. Schramm, and J. P. Kinzer (1946), High Q resonant cavities for microwave testing, Bell Syst. Techn. J. 25, 408-434.

APPENDIX A. SPS POWER DENSITY PATTERN AT RECTENNA SITE
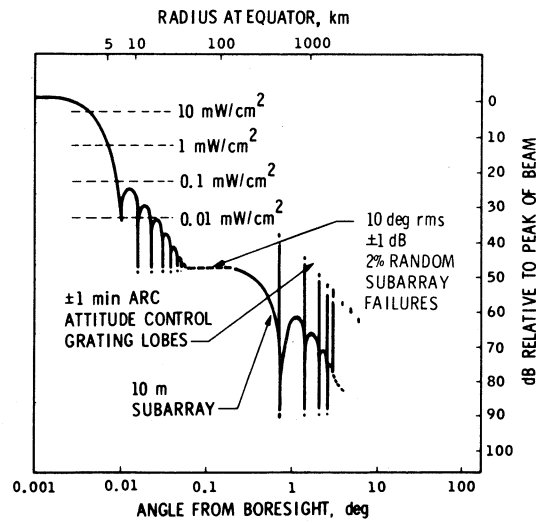
Figure A-1. Proposed SPS transmitted power
density pattern (Dickinson, 1978).

CIRCULAR ARRAY 1 km DIA.

6.5 GW AT 2450 MHz

10.0 dB GAUSSIAN TAPER

UNIFORM SQUARE ELEMENTS, 10 m

CODE:	dB	mW/cm^2
A	0	20
B	-3	10
C	-10	2
D	-16	0.5
E	-25	0.063
F	-30	0.02
G	-35	0.0063
H	-40	0.002
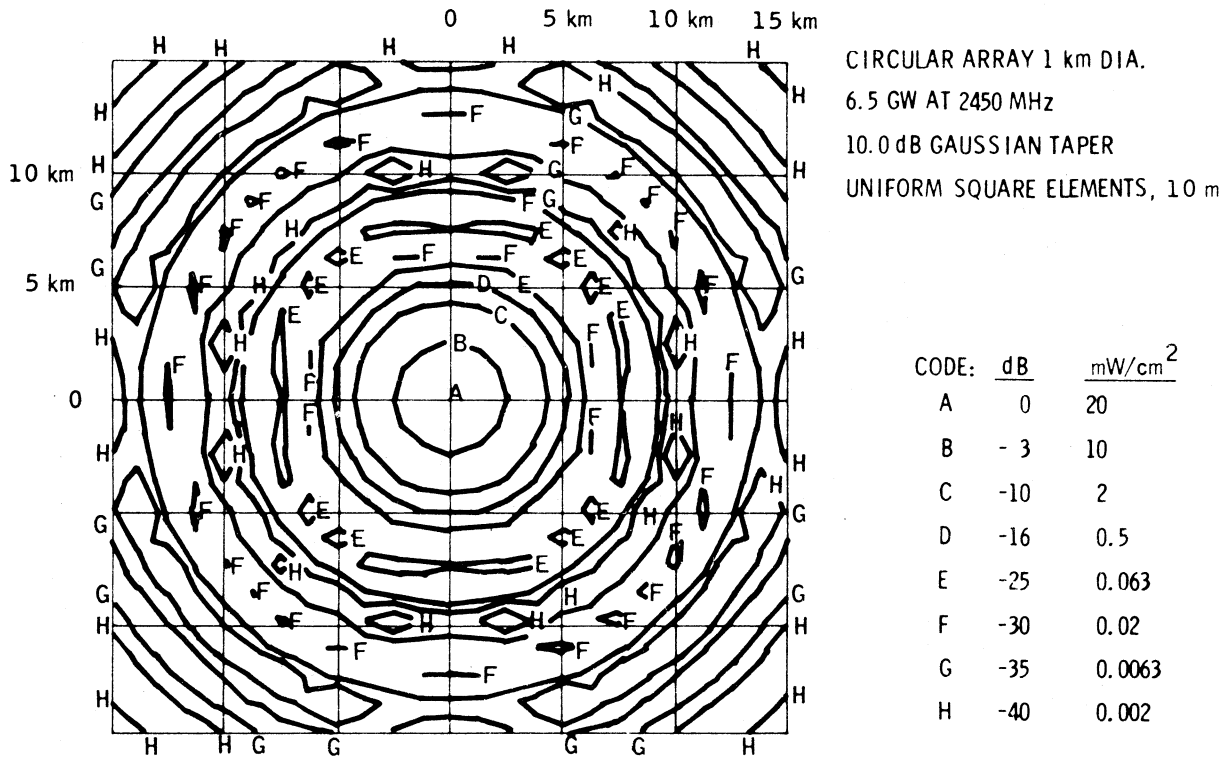
Figure A-2. Microwave power distribution on
rectenna at equator (Dickinson, 1978).

APPENDIX B. FORMULAS FOR THREE SIMPLE TYPES OF CAVITY RESONATORS
(Kinzer and Wilson, 1947)

← ———————————————— Field Components ———————————————— →

TYPE OF CAVITY & CO-ORDINATE SYSTEM	MODE	FIELD EQUATIONS *	DEFINITIONS	RESTRICTIONS ON ℓ, m, n
RECTANGULAR PRISM	TM	$E_x = \sqrt{\frac{\mu}{\epsilon}} \frac{k_1 k_3}{k^2} \cos k_1 x \, \sin k_2 y \, \sin k_3 z$ $E_y = \sqrt{\frac{\mu}{\epsilon}} \frac{k_2 k_3}{k^2} \sin k_1 x \, \cos k_2 y \, \sin k_3 z$ $E_z = -\sqrt{\frac{\mu}{\epsilon}} \frac{k_1^2 + k_2^2}{k^2} \sin k_1 x \, \sin k_2 y \, \cos k_3 z$ $H_x = -\frac{k_2}{k} \sin k_1 x \, \cos k_2 y \, \cos k_3 z$ $H_y = \frac{k_1}{k} \cos k_1 x \, \sin k_2 y \, \cos k_3 z$ $H_z = 0$	$k_1 = \frac{\ell \pi}{a} \quad k_2 = \frac{m \pi}{b} \quad k_3 = \frac{n \pi}{L}$ $k^2 = k_1^2 + k_2^2 + k_3^2 \quad \lambda = \frac{2\pi}{k}$ ℓ, m, n = INTEGRAL INDICES IDENTIFYING THE MODES. MAY ASSUME THE VALUE ZERO, SUBJECT TO RESTRICTIONS GIVEN IN ADJOINING COLUMN	$\ell > 0$ $m > 0$
	TE	$E_x = -\sqrt{\frac{\mu}{\epsilon}} \frac{k_2}{k} \cos k_1 x \, \sin k_2 y \, \sin k_3 z$ $E_y = \sqrt{\frac{\mu}{\epsilon}} \frac{k_1}{k} \sin k_1 x \, \cos k_2 y \, \sin k_3 z$ $E_z = 0$ $H_x = \frac{k_1 k_3}{k^2} \sin k_1 x \, \cos k_2 y \, \cos k_3 z$ $H_y = \frac{k_2 k_3}{k^2} \cos k_1 x \, \sin k_2 y \, \cos k_3 z$ $H_z = -\frac{k_1^2 + k_2^2}{k^2} \cos k_1 x \, \cos k_2 y \, \sin k_3 z$		$\ell + m > 0$ $n > 0$
CIRCULAR CYLINDER	TM	$E_\rho = -\sqrt{\frac{\mu}{\epsilon}} \frac{k_3}{k} J'_\ell(k_1 \rho) \cos \ell \theta \, \sin k_3 z$ $E_\theta = \sqrt{\frac{\mu}{\epsilon}} \ell \frac{k_3}{k} \frac{J_\ell(k_1 \rho)}{k_1 \rho} \sin \ell \theta \, \sin k_3 z$ $E_z = \sqrt{\frac{\mu}{\epsilon}} \frac{k_1}{k} J_\ell(k_1 \rho) \cos \ell \theta \, \cos k_3 z$ $H_\rho = -\ell \frac{J_\ell(k_1 \rho)}{(k_1 \rho)} \sin \ell \theta \, \cos k_3 z$ $H_\theta = -J'_\ell(k_1 \rho) \cos \ell \theta \, \cos k_3 z$ $H_z = 0$	$k_1 = \frac{2 r_{\ell m}}{a} \quad k_3 = \frac{n \pi}{L}$ $k^2 = k_1^2 + k_3^2 \quad \lambda = \frac{2\pi}{k}$ ℓ, m, n = DEFINED AS FOR RECTANGULAR PRISM $r_{\ell m}$ = m^{th} ZERO OF $J_\ell(x)$ FOR TM MODES $r_{\ell m}$ = m^{th} ZERO OF $J'_\ell(x)$ FOR TE MODES	$m > 0$
	TE	$E_\rho = -\sqrt{\frac{\mu}{\epsilon}} \ell \frac{J_\ell(k_1 \rho)}{k_1 \rho} \sin \ell \theta \, \sin k_3 z$ $E_\theta = -\sqrt{\frac{\mu}{\epsilon}} J'_\ell(k_1 \rho) \cos \ell \theta \, \sin k_3 z$ $E_z = 0$ $H_\rho = \frac{k_3}{k} J'_\ell(k_1 \rho) \cos \ell \theta \, \cos k_3 z$ $H_\theta = -\ell \frac{k_3}{k} \frac{J_\ell(k_1 \rho)}{k_1 \rho} \sin \ell \theta \, \cos k_3 z$ $H_z = \frac{k_1}{k} J_\ell(k_1 \rho) \cos \ell \theta \, \sin k_3 z$		$m > 0$ $n > 0$
FULL COAXIAL $\frac{b}{a} = \eta$	TM	SAME AS FOR CIRCULAR CYLINDER, BUT SUBSTITUTE: $Z_\ell(k_1 \rho)$ FOR $J_\ell(k_1 \rho)$ $Z'_\ell(k_1 \rho)$ FOR $J'_\ell(k_1 \rho)$ WHERE	SAME AS CIRCULAR CYLINDER, EXCEPT: $r_{\ell m}$ = m^{th} ZERO OF $[J_\ell(\eta x) Y_\ell(x) - J_\ell(x) Y_\ell(\eta x)]$ $A = \frac{J_\ell(r_{\ell m})}{Y_\ell(r_{\ell m})}$ FOR TM MODES	$m > 0$ SPECIAL CASE OF TM 0,0,n MODE, WITH $r_{\ell m} = 0$
	TE	$Z_\ell(k_1 \rho) = J_\ell(k_1 \rho) - A Y_\ell(k_1 \rho)$ $Z'_\ell(k_1 \rho) = J'_\ell(k_1 \rho) - A Y'_\ell(k_1 \rho)$	$r_{\ell m}$ = m^{th} ZERO OF $[J'_\ell(\eta x) Y'_\ell(x) - J'_\ell(x) Y'_\ell(\eta x)]$ $A = \frac{J'_\ell(r_{\ell m})}{Y'_\ell(r_{\ell m})}$ FOR TE MODES	$m > 0$ $n > 0$
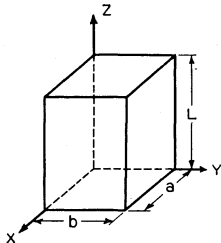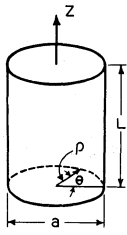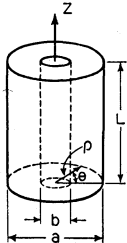
SOURCES: HANSEN, JNL. APP. PHYS., 9, P.654   BORGNIS, HOCHF: TECH u. ELEK: AKUS., 56, P.47
BORGNIS, ANN. d. PHYS., 35, P.359   BARROW & MIEHER, PROC. I.R.E., 28, P.184

* THE TIME FACTOR HAS BEEN OMITTED; THE E-FIELD IS IN TIME QUADRATURE WITH THE H-FIELD, WITH $\omega = ck$

Resonances	Mode Density	Q-factor Calculation	
NORMAL WAVELENGTHS	APPROXIMATION FOR TOTAL NUMBER OF MODES (TE & TM) HAVING $\lambda > \lambda_0$	FORMULAS FOR $Q\frac{\delta}{\lambda}$	DEFINITIONS

Row 1:

$$\lambda = \frac{2}{\sqrt{\left(\frac{\ell}{a}\right)^2 + \left(\frac{m}{b}\right)^2 + \left(\frac{n}{L}\right)^2}}$$

SAME AS TM MODES

$$N = 8.38\,\frac{V}{\lambda_0^3} - \frac{P}{\lambda_0}$$

$$V = abL$$

$$P = a+b+L$$

$$\frac{abL}{4} \cdot \frac{(p^2+q^2)(p^2+q^2+r^2)^{\frac{1}{2}}}{p^2 b(a+L) + q^2 a(b+L)} \qquad n > 0$$

$$\frac{abL}{2} \cdot \frac{(p^2+q^2)^{\frac{3}{2}}}{p^2 b(a+2L) + q^2 a(b+2L)} \qquad n = 0$$

$$\frac{abL}{4} \cdot \frac{(p^2+q^2)(p^2+q^2+r^2)^{\frac{3}{2}}}{aL\left[p^2 r^2 + (p^2+q^2)^2\right] + bL\left[q^2 r^2 + (p^2+q^2)^2\right] + ab\,r^2(p^2+q^2)} \qquad \ell m > 0$$

$$\frac{abL}{2} \cdot \frac{(q^2+r^2)^{\frac{3}{2}}}{q^2 L(b+2a) + r^2 b(L+2a)} \qquad \ell = 0$$

$$\frac{abL}{2} \cdot \frac{(p^2+r^2)^{\frac{3}{2}}}{p^2 L(a+2b) + r^2 a(L+2b)} \qquad m = 0$$

$$p = \frac{\ell}{a}$$
$$q = \frac{m}{b}$$
$$r = \frac{n}{L}$$

Row 2:

$$\lambda = \frac{2}{\sqrt{\left(\frac{2r_{\ell m}}{\pi a}\right)^2 + \left(\frac{n}{L}\right)^2}}$$

$$(fa)^2 = \left(\frac{c\,r_{\ell m}}{\pi}\right)^2 + \left(\frac{cn}{2}\right)^2 \left(\frac{a}{L}\right)^2$$

$c = \sqrt{\mu\epsilon}$ = VELOCITY OF ELECTROMAGNETIC WAVES IN DIELECTRIC

f = FREQUENCY

$$N = 4.38\,\frac{V}{\lambda_0^3} + 0.09\,\frac{S}{\lambda_0^2}$$

$$V = \frac{\pi a^2 L}{4}$$

$$S = \pi a L$$

$$\frac{r_{\ell m}}{2\pi}\left[1 + p^2 R^2\right]^{\frac{1}{2}} \cdot \frac{1}{1+R} \qquad n > 0$$

$$\frac{r_{\ell m}}{\pi}\,\frac{1}{2+R} \qquad n = 0$$

$$\frac{r_{\ell m}}{2\pi}\left[1 + p^2 R^2\right]^{\frac{3}{2}} \frac{1 - \left(\frac{\ell}{r_{\ell m}}\right)^2}{1 + p^2 R^3 + p^2(1-R)R^2\left(\frac{\ell}{r_{\ell m}}\right)^2}$$

$$R = \frac{a}{L}$$
$$p = \frac{n\pi}{2r_{\ell m}}$$

Row 3:

SAME FORM AS FOR CYLINDER

$r_{\ell m}$ HAS DIFFERENT VALUES

$$N \approx 4.4\,\frac{V}{\lambda_0^3}$$

WITH SOME DOUBT AS TO VALUE OF THE COEFFICIENT

$$\frac{r_{\ell m}}{2\pi}\left[1 + p^2 R^2\right]^{\frac{1}{2}} \frac{(1 - \eta^2 H')}{(1 + \eta H') + R(1 - \eta^2 H')} \qquad n > 0$$

$$\frac{r_{\ell m}}{\pi} \cdot \frac{(1 - \eta^2 H')}{2(1 + \eta H') + R(1 - \eta^2 H')} \qquad n = 0$$

THESE EXPRESSIONS ARE NOT VALID FOR SMALL η WHEN $\ell = 0$

$$\frac{r_{\ell m}}{2\pi} \cdot \frac{\left[1 + p^2 R^2\right]^{\frac{3}{2}} M}{(1 + \eta H) + p^2 R^2 \frac{\ell^2}{r_{\ell m}^2}\left(1 + \frac{H}{\eta}\right) + p^2 R^3 M}$$

WHERE

$$M = \left(1 - \frac{\ell^2}{r_{\ell m}^2}\right) - \eta^2 H\left(1 - \frac{\ell^2}{\eta^2 r_{\ell m}^2}\right)$$

$$R = \frac{a}{L}$$
$$p = \frac{n\pi}{2r_{\ell m}}$$
$$H' = \left[\frac{Z'_\ell(\eta\,r_{\ell m})}{Z'_\ell(r_{\ell m})}\right]^2$$
$$H = \left[\frac{Z_\ell(\eta\,r_{\ell m})}{Z_\ell(r_{\ell m})}\right]^2$$

BIBLIOGRAPHIC DATA SHEET

	1. PUBLICATION NO. NTIA Report 80-49	2. Gov't Accession No.	3. Recipient's Accession No.
4. TITLE AND SUBTITLE Field Maxima Inside Habitable Structures Exposed to 2.45 GHz Plane Wave Radiation			5. Publication Date **October 1980**
			6. Performing Organization Code
7. AUTHOR(S) Hans J. Liebe			9. Project/Task/Work Unit No. 910 4422
8. PERFORMING ORGANIZATION NAME AND ADDRESS National Telecommunications & Information Administration Institute for Telecommunication Sciences 1-3449 325 Broadway Boulder, CO 80303			
			10. Contract/Grant No.
11. Sponsoring Organization Name and Address Department of Energy Washington, D.C. 20545			12. Type of Report and Period Covered
			13.

14. SUPPLEMENTARY NOTES

15. ABSTRACT *(A 200-word or less factual summary of most significant information. If document includes a significant bibliography or literature survey, mention it here.)*

This report discusses microwave engineering data relevant to assess the potential of the Satellite Power System (SPS) to cause microwave field enhancements (so-called "hot spots") inside habitable structures (house, trailer, car, etc.) located in the fringe area of the receiving rectenna. Mitigative measures are included in the discussion.

16. Key Words *(Alphabetical order, separated by semicolons)*

17. AVAILABILITY STATEMENT ☒ UNLIMITED. ☐ FOR OFFICIAL DISTRIBUTION.	18. Security Class. *(This report)* UNCLASSIFIED	20. Number of pages 37
	19. Security Class. *(This page)* UNCLASSIFIED	21. Price: